

r.sim.terrain: a dynamic landscape evolution model

Brendan Alexander Harmon^{1,2}, Helena Mitasova^{1,3}, Anna Petrasova^{1,3}, and Vaclav Petras^{1,3}

¹Center for Geospatial Analytics, North Carolina State University, Raleigh, North Carolina, United States of America

²Robert Reich School of Landscape Architecture, Louisiana State University, Baton Rouge, Louisiana

³Department of Marine, Earth, and Atmospheric Sciences, North Carolina State University, Raleigh, North Carolina, United States of America

Correspondence: Brendan Harmon (brendan.harmon@gmail.com)

Abstract. While there are numerical landscape evolution models that simulate how steady state flows of water and sediment reshape topography over long periods of time, this is the first to simulate short-term topographic change for both steady state and dynamic flow regimes. It is a process-based, spatially distributed model that uses the water and sediment flow continuity equations to simulate how overland sediment mass flows reshape topography. This either steady state or dynamic model can

5 simulate how topography will evolve for a range of hydrologic soil erosion regimes based on topographic, land cover, soil, and rainfall parameters. A case study demonstrates how the behavior and results of the dynamic model differ the steady state model. The dynamic model is more accurate and demonstrates cross-scale interactions between topographic form and sediment flow processes.

Copyright statement. ...

10 1 Introduction

Landscape evolution models represent how the surface of the earth changes over time. Most studies of landscape evolution have been descriptive, but a number of numerical landscape evolution models have been developed that simulate elevational change over time (Temme et al., 2013). Numerical landscape evolution models such as the Channel-Hillslope Integrated Landscape Development (CHILD) model (Tucker et al., 2001) and SIBERIA (Willgoose, 2005) simulate steady state flows over 15 long temporal scales. Landlab,¹ a new Python library for numerically modeling Earth surface processes (Hobley et al., 2017), has components for simulating landscape evolution such as the Stream Power with Alluvium Conservation and Entrainment (SPACE) model (Shobe et al., 2017). There are still, however, major research questions to address in the theoretical foundations of erosion modeling such as how erosional processes scale over time and space and how sediment detachment and transport interact (Mitasova et al., 2013). A dynamic landscape evolution model is needed to study fine-scale spatial and short-term temporal erosional processes such as gully formation and the development of microtopography. While most numerical landscape

¹<http://landlab.github.io/>

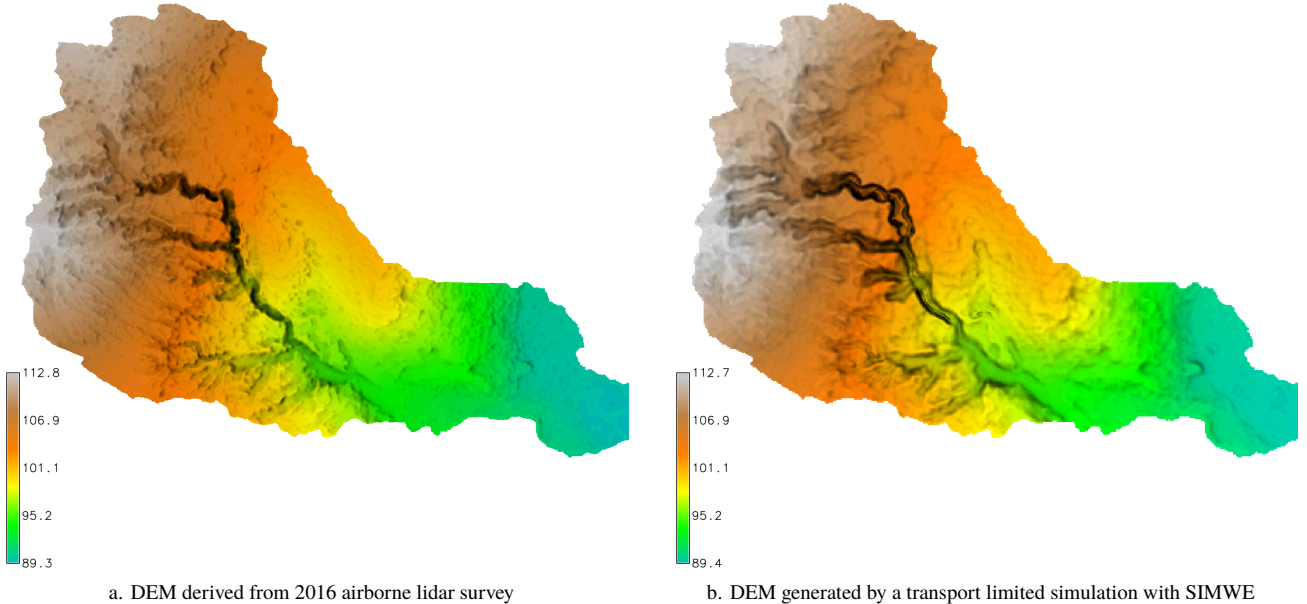


Figure 1. The digital elevation model (DEM) before (a.) and after (b.) simulated landscape evolution with r.sim.terrain. This simulation used the SIMWE model for a 120 *min* rainfall event with 25 mm hr^{-1} in a transport limited soil erosion regime at steady state. In the evolved DEM (b.) the gully channel has widened with depositional ridges forming along its centerline.

evolution models simulate peak flows at steady state (see Table 2), short-term erosional processes like gully formation can be dynamic with significant morphological changes happening within minutes before flows reach steady state.

At the beginning of a rainfall event the overland water flow regime is dynamic – its depth changes at a variable rate over time and space. If the intensity of rainfall continues to change throughout the event then the flow regime will remain dynamic. If, 5 however, the overland flow reaches a peak rate then the hydrologic regime is considered to be at steady state. At steady state:

$$\frac{\partial h(x, y, t)}{\partial t} = 0 \quad (1)$$

where:

(x, y) is the position (m)

t is the time (s)

10 $h(x, y, t)$ is the depth of overland flow (m)

Gullies are eroded, steep banked channels formed by ephemeral, concentrated flows of water. A gully forms when overland waterflow converges in a knickzone – a concave space with steeper slopes than its surroundings – during intense rainfall events. When the force of the water flow concentrated in the knickzone is enough to detach and transport large amounts of sediment,

an incision begins to form at the apex of the knickzone – the knickpoint or headwall. As erosion continues the knickpoint begins to migrate upslope and the nascent gully channel widens, forming steep channel banks. Multiple incisions initiated by different knickpoints may merge into a gully channel and multiple channels may merge into a branching gully system. This erosive process is dynamic; the morphological changes drive further changes in a positive feedback loop until water flow

- 5 reaches steady state. When the gully initially forms the soil erosion regime should be detachment capacity limited with the concentrated flow of water in the channel of the gully detaching large amounts of sediment and transporting it to the foot of the gully, potentially forming a depositional fan. After the initial formation of the gully the soil erosion regime may change. If the intensity of the rainfall decreases the regime may switch to erosion-deposition. Subsequent rainfall events may trigger further knickpoint formation and upslope migration, channel incision and widening, and depositional fan and ridge formation.
- 10 Between high intensity rainfall events, lower intensity events and gravitational diffusion may gradually smooth the shape of the gully. Eventually, if detachment capacity significantly exceeds transport capacity, the gully may fill with sediment.

Gully erosion rates and evolution can be monitored in the field or modeled on the computer. Field methods include dendrogeomorphology (Malik, 2008) and permanent monitoring stakes for recording erosion rates, extensometers for recording mass wasting events, weirs for recording water and suspended sediment discharge rates, and time series of surveys using total
15 station theodolites (Thomas et al., 2004), unmanned aerial systems (UAS), airborne lidar, and terrestrial lidar (Starek et al., 2011; Bechet et al., 2016).

With terrestrial lidar, airborne lidar and UAS photogrammetry there is now high enough resolution topographic data to morphometrically analyze and numerically model fine-scale landscape evolution in GIS including processes such as gully formation and the development of microtopography. Gully erosion has been simulated with the Revised Universal Soil Loss
20 Equation Version 2 (RUSLER) in conjunction with the Ephemeral Gully Erosion Estimator (EphGEE) (Dabney et al., 2014), while gully evolution has been simulated for detachment capacity limited erosion regimes with the Simulation of Water Erosion (SIMWE) model (Koco, 2011; Mitasova et al., 2013). Now numerical landscape evolution models that can simulate steady state and dynamic flow regimes and can dynamically switch between soil erosion regimes are needed to study fine-scale spatial and short-term temporal erosional processes.

25 The numerical landscape evolution model r.sim.terrain was developed to simulate the spatiotemporal evolution of landforms caused by shallow overland water and sediment flows at spatial scales ranging from square meters to thousands of kilometers and temporal scales ranging from minutes to years. This open source, GIS-based landscape evolution model can simulate either steady state or dynamic flow regimes, dynamically switch between soil erosion regimes, and simulate the evolution of fine-scale morphological features such as ephemeral gullies (Figure 1). It was designed as a research tool for studying how
30 erosional processes scale over time and space, comparing empirical and process-based models, comparing steady state and dynamic flow regimes, and studying the role of dynamic flow regimes in fine-scale morphological change. r.sim.terrain was tested with a regional scale (650km^2) case study and a subwatershed scale (450m^2) case study. At the subwatershed scale simulations were compared against a time-series of lidar surveys.

2 r.sim.terrain

r.sim.terrain is a process-based, spatially distributed landscape evolution model that simulates topographic changes caused by shallow, overland water flow across a range of spatiotemporal scales and soil erosion regimes using either the Simulated Water Erosion (SIMWE) model, the 3-Dimensional Revised Universal Soil Loss Equation (RUSLE 3D) model, or the Unit Stream

5 Power Erosion Deposition (USPED) model. SIMWE is a physics-based simulation that uses a Monte Carlo path sampling method to solve the water and sediment flow equations for detachment limited, transport limited, and erosion-deposition soil erosion regimes (Mitasova et al., 2004). With SIMWE r.sim.terrain uses the modeled flow of sediment – a function of water flow and soil detachment and transport parameters – to estimate the net erosion and deposition rates. RUSLE3D is an empirical equation for sediment flows in detachment capacity limited soil erosion regimes (Mitasova et al., 1996). With RUSLE3D
10 r.sim.terrain uses an event-based erosivity factor, the slope, the flow accumulation, and a 3D topographic factor to model sediment flow. USPED is an empirical equation for net erosion and deposition in transport capacity limited soil erosion regimes. With USPED r.sim.terrain uses an event-based erosivity factor, the slope and aspect, the flow accumulation, and a 3D topographic factor to model erosion-deposition as the divergence of sediment flows. For each of the models topographic change
15 is derived at each time step from the sediment flow or net erosion-deposition rate and gravitational diffusion. r.sim.terrain can simulate steady state or dynamic flow regimes. During simulations with SIMWE r.sim.terrain can switch between detachment limited, transport limited, and erosion-deposition soil erosion regimes.

r.sim.terrain can simulate the evolution of gullies including processes such as knickpoint migration, channel incision, channel widening, and scour pool and depositional riffle formation along the thalweg of the gully. Applications include geomorphological research, erosion control, landscape restoration, and scenario development for landscape planning and management.

20 r.sim.terrain can simulate landscape evolution over a wide range of spatial scales from small watersheds less than ten square kilometers with SIMWE to regional watersheds of thousands of square kilometers with USPED or RULSE3D.

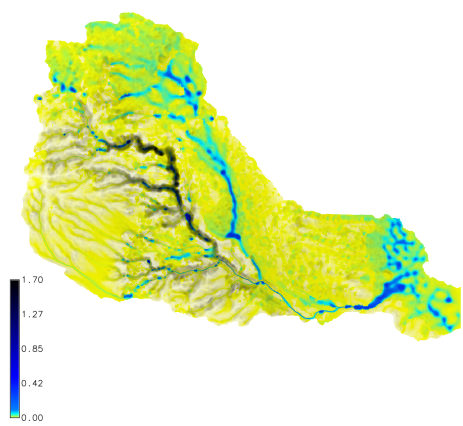
This model has been implemented as a Python add-on module for the free, open source Geographic Resources Analysis Support System (GRASS) GIS². The source code is available at https://github.com/baharmon/landscape_evolution under the GNU General Public License v2. This highly adaptable geographic information system (GIS)-based implementation was developed
25 as a research tool for studying the interaction of sediment detachment and transport and the scaling of erosional processes over time and space. It supports multithreading and parallel processing to efficiently compute simulations using large, high resolution topographic datasets. The landscape evolution model can be installed in GRASS GIS as an add-on module with the command:

```
g.extension r.sim.terrain url=github.com/baharmon/landscape_evolution
```

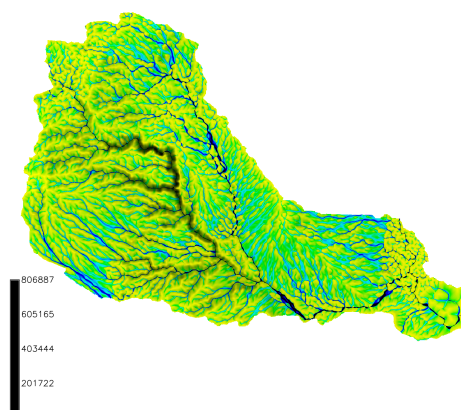
30 2.1 Simulation of water erosion model

SIMWE – the Simulation of Water Erosion model – is a physics-based simulation of shallow overland water and sediment flow that uses a path sampling method to solve the continuity and momentum equations with a 2D diffusive wave approximation

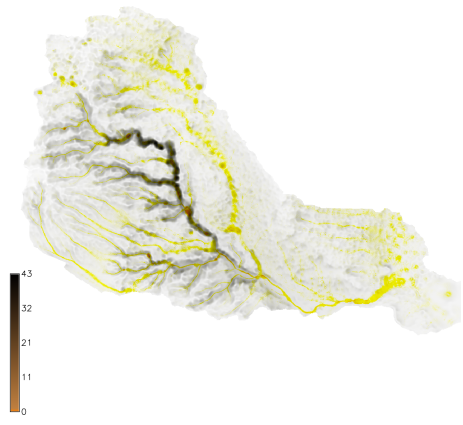
²<https://grass.osgeo.org/>



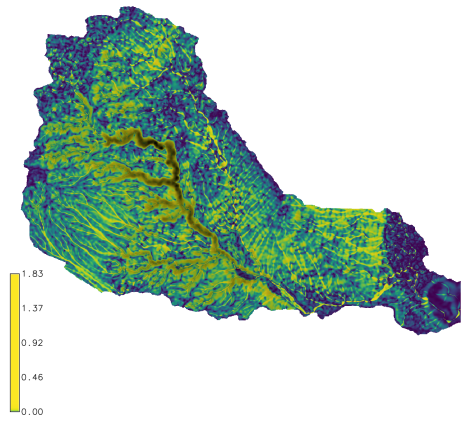
a. Water depth (m) simulated by SIMWE



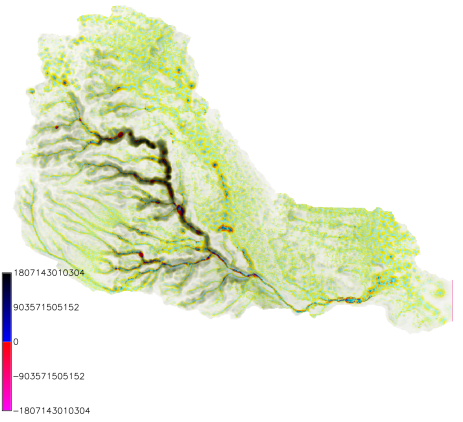
d. Flow accumulation for RUSLE3D



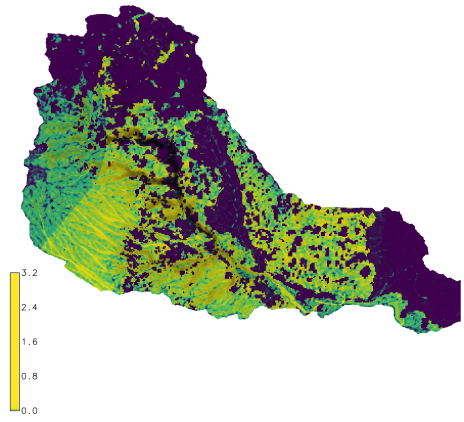
b. Sediment flux ($\text{kg m}^{-1} \text{s}^{-1}$) simulated by SIMWE



e. LS3D topographic factor for RUSLE3D



c. Erosion and deposition ($\text{kg m}^{-2} \text{s}^{-1}$) simulated by SIMWE



f. Sediment flow modeled by RUSLE3D ($\text{kg m}^{-2} \text{s}^{-1}$)

Figure 2. Water and sediment flows simulated by SIMWE for a 10 min event with 50 mm hr^{-1} and by RUSLE3D with a R-factor of 310

Table 1. GIS-based soil erosion models

Model	Spatial scale	Temporal scale	Representation	Implementation	Reference
GeoWEPP	watershed	continuous	raster	ArcGIS module	(Dennis C. Flanagan et al., 2013)
AGWA	watershed	event –	vector	ArcGIS module	(Guertin et al., 2015)
		continuous			
RUSLE3D	regional	continuous	raster	map algebra	(Mitasova et al., 1996)
USPED	watershed	continuous	raster	map algebra	(Mitasova et al., 1996)
SIMWE	watershed	event –	raster	GRASS modules	(Mitas and Mitasova, 1998)
		continuous			

Table 2. Numerical landscape evolution models

Model	Spatial scale	Temporal scale	Representation	Dynamics	Implementation	Reference
SIBERIA	regional	continuous	raster	steady state	Fortran prog.	(Willgoose, 2005)
CHILD	regional	continuous	mesh	steady state	C++ program	(Tucker et al., 2001)
Landlab	regional	continuous	raster + mesh	steady state	Python library	(Hobley et al., 2017)
r.landscape.evol	regional	continuous	raster	steady state	GRASS module	(Barton et al., 2010)
r.sim.terrain	watershed –	event –	raster	dynamic –	GRASS module	
	regional	continuous		steady state		

(Mitas and Mitasova, 1998; Mitasova and Mitas, 2001; Mitasova et al., 2004). It has been implemented in GRASS GIS as the modules r.sim.water³ and r.sim.sediment⁴.

In SIMWE mode for each time step r.sim.terrain determines the soil erosion regime, simulates water and sediment flows, and then evolves the topography. In an erosion-deposition regime the model computes the partial derivatives of the topography, 5 simulates shallow water flow and erosion-deposition, and then evolves the topography based on the erosion-deposition rate and gravitational diffusion. The same process is used in a transport capacity limited regime except that the topography is evolved based on the transport limited erosion-deposition rate and gravitational diffusion. In a detachment capacity limited regime the model instead computes the partial derivatives of the topography, simulates shallow water flow and sediment flow, and then evolves the topography based on the sediment flow rate and gravitational diffusion. The model simulates dynamic landscape 10 evolution when the time step is less than the travel time for a drop of water or a particle of sediment to cross the landscape. With longer time steps the model simulates steady state dynamics.

³<https://grass.osgeo.org/grass75/manuals/r.sim.water.html>

⁴<https://grass.osgeo.org/grass75/manuals/r.sim.sediment.html>

2.1.1 Erosion regime

This model can switch erosion regimes at each time step based on the rainfall intensity i_r and the balance of the sediment detachment capacity D_c and the sediment transport capacity T_c represented by the first order reaction term σ which depends on soil and landcover properties. The detachment capacity is the maximum potential detachment rate by overland

5 flow, while the sediment transport capacity is the maximum potential sediment flow rate. When rainfall intensity is very high ($i_r \geq 60\text{mm hr}^{-1}$) or σ is low ($\sigma \leq 0.01\text{m}^{-1}$), then the regime is detachment capacity limited. When rainfall intensity is not very high ($i_r < 60\text{mm hr}^{-1}$) and σ is high ($\sigma \geq 100\text{m}^{-1}$), then the regime is transport capacity limited. When rainfall intensity is not very high ($i_r < 60\text{mm hr}^{-1}$) and σ is neither high nor low ($0.01\text{m}^{-1} < \sigma < 100\text{m}^{-1}$), then there is an erosion-deposition regime.

10

$$\sigma = \frac{D_c}{T_c} \quad (2)$$

where:

σ is a first order reaction term (m^{-1})

D_c is the sediment detachment capacity ($\text{kg m}^{-1}\text{s}^{-1}$)

15 T_c is the sediment transport capacity ($\text{kg m}^{-1}\text{s}^{-1}$)

2.1.2 Shallow water flow

The SIMWE model simulates shallow overland water flow controlled by spatially variable topographic, soil, landcover, and rainfall parameters by solving the continuity and momentum equations for steady state water flow with a path sampling method

20 (Fig. 2a). Shallow water flow $q(x, y, t)$ can be approximated by the bivariate form of the St. Venant equation:

$$\frac{\partial h(x, y, t)}{\partial t} = i_e(x, y, t) - \nabla \cdot q(x, y, t) \quad (3)$$

where:

(x, y) is the position (m)

t is the time (s)

25 $h(x, y, t)$ is the depth of overland flow (m)

$i_e(x, y, t)$ is the rainfall excess (m s^{-1})

(i.e. rainfall intensity – infiltration – vegetation intercept)

∇ is the divergence of the flow vector field

$q(x, y, t)$ is the water flow per unit width ($\text{m}^2 \text{s}^{-1}$).

30

Diffusive wave effects can be approximated so that water can flow through depressions by integrating a diffusion term $\propto \nabla^2[h^{5/3}(x, y)]$ into the solution of the continuity and momentum equations for steady state water flow. This equation is

solved using a Green's function Monte Carlo path sampling method.

$$-\frac{\varepsilon(x,y)}{2} \nabla^2 [h^{5/3}(x,y)] + \nabla [h(x,y) v(x,y)] = i_e(x,y) \quad (4)$$

where:

$\varepsilon(x,y)$ is a spatially variable diffusion coefficient.

5

2.1.3 Sediment flow

In SIMWE the sediment flow rate $q_s(x,y,t)$ is estimated as a function of water flow and sediment concentration (Fig. 2b):

$$q_s(x,y,t) = \rho_s(x,y,t) q(x,y,t) \quad (5)$$

where:

10 $q_s(x,y,t)$ is the sediment flow rate per unit width ($kg\ m^{-1}s^{-1}$)

$\rho_s(x,y,t)$ is sediment mass density ($kg\ m^{-3}$).

2.1.4 Erosion-deposition

In SIMWE the net erosion-deposition rate is estimated using the bivariate form of sediment continuity equation to model 15 sediment storage and flow based on effective sources and sinks (Fig. 2c). Net erosion-deposition $d_s(x,y,t)$ – the difference between sources and sinks – is approximated by the steady state sediment flow equation with diffusion:

$$d_s(x,y,t) = \frac{\partial[\rho_s c(x,y,t) h(x,y,t)]}{\partial t} + \nabla q_s(x,y,t) \quad (6)$$

where:

$d_s(x,y,t)$ is net erosion-deposition ($kg\ m^{-2}s^{-1}$).

20

2.1.5 Landscape evolution

The simulated change in elevation $\Delta z(x,y,t)$ due to water erosion and deposition is a function of the change in time, the net 25 erosion-deposition rate, and the sediment mass density (Mitasova et al., 2013):

$$\Delta z(x,y,t) = \Delta t d_s(x,y,t) \rho_s^{-1} \quad (7)$$

25 In a detachment limited erosion regime the simulated change in elevation $\Delta z(x,y,t)$ is a function of the change in time, the sediment flow rate, and the mass of water carried sediment per unit area (Mitasova et al., 2013):

$$\Delta z(x,y,t) = \Delta t q_s(x,y,t) \varrho_s^{-1} \quad (8)$$

where:

ϱ_s is the mass of sediment per unit area ($kg\ m^{-2}$).

Gravitational diffusion is then applied to the evolved topography to simulate the settling of sediment particles. The simulated
5 change in elevation $\Delta z(x,y,t)$ due to gravitational diffusion is a function of the change in time, the sediment mass density,
the gravitational diffusion coefficient, and topographic divergence – i.e. the sum of the second order derivatives of elevation
(Thaxton, 2004):

$$\Delta z(x,y,t) = \Delta t \rho_s^{-1} \varepsilon_g \nabla(x,y,t) \quad (9)$$

where:

10 ε_g is the gravitational diffusion coefficient ($m^2 s^{-1}$)

$\nabla(x,y,t)$ is the topographic divergence (m^{-1}).

2.2 Revised universal soil loss equation 3D model

The Revised Universal Soil Loss Equation for Complex Terrain (RUSLE3D) is an empirical equation for computing erosion in
15 a detachment capacity limited soil erosion regime for watersheds with complex topography (Mitasova et al., 1996). It is based
on the Universal Soil Loss Equation (USLE), an empirical equation for estimating the average sheet and rill soil erosion from
rainfall and runoff on agricultural fields and rangelands with simple topography (Wischmeier et al., 1978). It models erosion
dominated regimes without deposition in which sediment transport capacity is uniformly greater than detachment capacity. As
an empirical equation the predicted soil loss is spatially and temporally averaged. In USLE soil loss per unit area is determined
20 by an erosivity factor R , a soil erodibility factor K , a slope length factor L , a slope steepness factor S , a cover management
factor C , and a prevention measures factor P . These factors are empirical constants derived from an extensive collection of
measurements on 22.13 m standard plots with an average slope of 9%. RUSLE3D was designed to account for more complex,
3D topography with converging and diverging flows. In RUSLE3D the topographic potential for erosion at any given point is
represented by a 3D topographic factor LS_{3D} , which is a function of the upslope contributing area and the angle of the slope.
25 In this spatially and temporally distributed model RUSLE3D is modified by the use of a event-based r-factor derived from
the rainfall intensity at each time step. For each time step this model computes the parameters for RUSLE3D – an event-
based erosivity factor, the slope of the topography, the flow accumulation, and the 3D topographic factor – and then solves the
RUSLE3D equation for sediment flow. The sediment flow is used to simulate landscape evolution in a detachment capacity
limited soil erosion regime.

30 2.2.1 Event-based erosivity factor

In USLE and RUSLE the erosivity factor R is the combination of the total energy and peak intensity of a rainfall event,
representing the interaction between the detachment of sediment particles and the transport capacity of the flow. It can be

calculated as the product of the the kinetic energy of the rainfall event E and its maximum 30-minute intensity I_{30} (Brown and Foster, 1987; Renard et al., 1997). In this model, however, the erosivity factor is derived at each time step as a function of kinetic energy, rainfall volume, rainfall intensity, and time. First rain energy is derived from rainfall intensity (Brown and Foster, 1987):

$$5 \quad e_r = 0.29 (1. - 0.72 \exp(-0.05 i_r)) \quad (10)$$

where:

e_r is unit rain energy ($MJ ha^{-1} mm^{-1}$)

i_r is rainfall intensity ($mm h^{-1}$).

- 10 Then the event-based erosivity index R_e is calculated as the product of unit rain energy, rainfall volume, rainfall intensity, and time:

$$R_e = e_r v_r i_r t_r \quad (11)$$

R_e is the event-based erosivity index ($MJ mm ha^{-1} hr^{-1}$)

v_r is rainfall volume (mm) derived from $v_r = i_r t_r$

- 15 t_r is time interval s

2.2.2 Flow accumulation

The upslope contributing area is determined by flow accumulation (Fig. 2d). Flow accumulation is calculated using a multiple flow direction algorithm (Metz et al., 2009) based on A^T least cost path searches (Ehlschlaeger, 1989). The multiple flow direction algorithm implemented in GRASS GIS as the module *r.watershed*⁵ is computationally efficient and can navigate nested depressions and other obstacles.

2.2.3 3D topographic factor

The 3D topographic factor $LS_{3D}(x, y)$ is calculated as a function of the flow accumulation, representing the upslope contributing area, and the slope (Fig. 2e). The empirical coefficients m and n for the upslope contributing area and the slope can range 25 from 0.2 to 0.6 and 1.0 to 1.3 respectively with low values representing dominant sheet flow and high values representing dominant rill flow.

$$LS_{3D}(x, y) = (m + 1.0) (a(x, y) a_0^{-1})^m (\sin(\beta) \beta_0^{-1})^n \quad (12)$$

where:

LS_{3D} is the dimensionless topographic (length-slope) factor

⁵<https://grass.osgeo.org/grass72/manuals/r.watershed.html>

a is flow accumulation (m)

a_0 is the length of the standard USLE plot ($22.1m$)

β is the slope angle ($^\circ$)

m is an empirical coefficient

5 n is an empirical coefficient

β_0 is the slope of the standard USLE plot (0.09°)

2.2.4 Sediment flow

The sediment flow is a function of the event-based erosivity factor, the soil erodibility factor, the 3D topographic factor, cover

10 factor, and the prevention measures factor (Fig. 2f).

$$E = R_e K LS_{3D} C P \quad (13)$$

where:

E is soil loss ($kg\ m^{-2}\ min^{-1}$)

R_e is the event-based erosivity factor ($MJ\ mm\ ha^{-1}\ hr^{-1}$)

15 K is the soil erodibility factor ($ton\ ha\ hr\ ha^{-1}\ MJ^{-1}\ mm^{-1}$)

LS_{3D} is the dimensionless topographic (length-slope) factor

C is the dimensionless land cover factor

P is the dimensionless prevention measures factor

20 With RUSLE3D the simulated change in elevation $\Delta z(x, y, t)$ is derived from equation 8 for landscape evolution in an detachment limited soil erosion regime and then equation 9 for the settling of sediment particles due to gravitational diffusion.

2.3 Unit strempower erosion deposition model

The Unit Stream Power Erosion Deposition (USPED) model estimates net erosion-deposition as the divergence of sediment

25 flow in transport capacity limited soil erosion regimes. At transport capacity shallow flows of water are carrying as much

sediment possible – more sediment is being detached than can be transported. As a transport capacity limited model USPED

predicts erosion where transport capacity increases and deposition where transport capacity decreases. In USPED the influence

of topography on erosion and deposition is represented by a topographic sediment transport factor, while the influence of soil

and landcover are represented by factors adopted from USLE and RUSLE (Mitasova et al., 1996).

With USPED net erosion-deposition is estimated by computing the event-based erosivity factor R_e using Eq. 11, the slope
30 and aspect of the topography, the flow accumulation with a multiple flow direction algorithm, the topographic sediment trans-
port factor, the sediment flow at transport capacity, and the divergence of the sediment flow.

For USPED the 3D topographic factor (Eq. 12 for RUSLE3D is adapted to represent the topographic sediment transport factor LST – the topographic component of overland flow at sediment transport capacity:

$$LST = U^m (\sin \beta)^n \quad (14)$$

where:

- 5 LST is the topographic sediment transport factor
- U is the flow accumulation (m)
- β is the angle of the slope ($^\circ$)
- m is an empirical coefficient
- n is an empirical coefficient.

10

The sediment flow at transport capacity is a function of the event-based rainfall factor, the soil erodibility factor, the topographic component of overland flow, the landcover factor, and the prevention measures factor:

$$T = R_e K C P LST \quad (15)$$

where:

- 15 T is sediment flow at transport capacity ($kg m^{-1} s^{-1}$)
- R_e is the event-based rainfall factor ($MJ mm ha^{-1} hr^{-1}$)
- K is the soil erodibility factor ($ton ha hr ha^{-1} MJ^{-1} mm^{-1}$)
- C is the dimensionless land cover factor
- P is the dimensionless prevention measures factor.

20

Net erosion-deposition at transport capacity is estimated as the divergence of sediment flow:

$$d_s(x, y, t) = \frac{\partial(T \cos \alpha)}{\partial x} + \frac{\partial(T \sin \alpha)}{\partial y} \quad (16)$$

where:

- $d_s(x, y, t)$ is net erosion-deposition ($kg m^{-2} s^{-1}$)
- 25 α is the aspect of the topography ($^\circ$).

With USPED the simulated change in elevation $\Delta z(x, y, t)$ is derived from equation 7 for landscape evolution and then equation 9 for the settling of sediment particles due to gravitational diffusion.

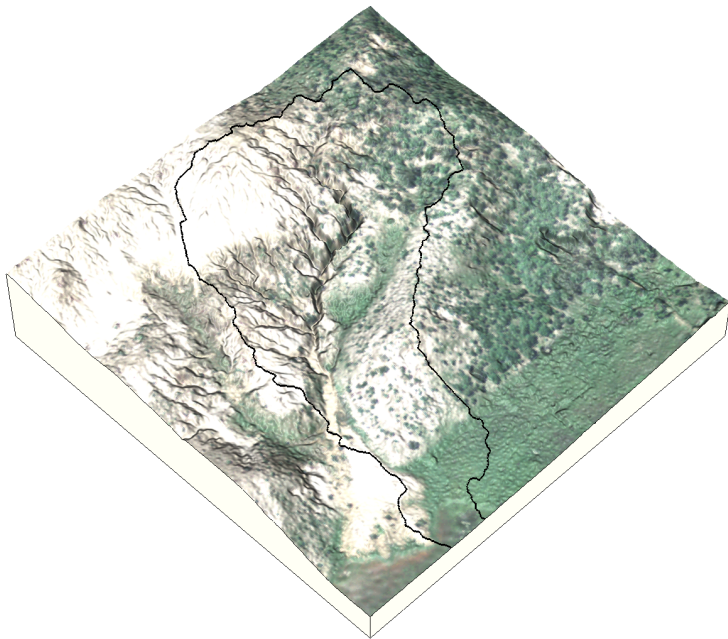


Figure 3. Subwatershed with 2014 orthoimagery draped over 2016 digital elevation model, Patterson Branch Creek, Fort Bragg, NC, USA

3 Case study

To test the effectiveness of r.sim.terrain's models we compared the simulated evolution of a highly eroded subwatershed of Patterson Branch Creek on Fort Bragg, North Carolina against a timeseries of lidar surveys. The models – SIMWE, RUSLE3D, and USPED – were tested in steady state and dynamic modes for constant rainfall, design storms, and recorded rainfall.

5 3.1 Patterson Branch Creek

Fort Bragg, a military installation in the Sandhills region of North Carolina with a Longleaf Pine and Wiregrass Ecosystem (Sorrie et al., 2006), has extensive areas of bare, erodible soils on impact areas, firing ranges, landing zones, and dropzones. The study landscape – a subwatershed of Patterson Branch Creek in the Coleman Impact Area – is pitted with impact craters from artillery and mortar shells and has an active, approximately 2 m deep gully. It is a Pine-Scrub Oak Sandhill community
10 composed primarily of Longleaf Pine – *Pinus palustris* – and Wiregrass – *Aristida stricta* – on Blaney and Gilead loamy sands (Sorrie, 2004). Throughout the Coleman Impact Area the frequent fires ignited by live munitions drive the ecological disturbance regime of this fire adapted ecosystem. In 2016 the 450 m^2 study site was 43.24% bare ground with predominately loamy sands, 39.54% covered by the Wiregrass community, and 17.22% forested with the Longleaf Pine community (Figure 4c).

We hypothesize that the elimination of forest cover in the impact zone triggered extensive channelized overland flow, gully formation, and sediment transport into the creek.

We generated a timeseries of digital elevations models and landcover maps of the study landscape from lidar pointclouds and orthophotography (Figure 4a-c). The digital elevations models for 2004, 2012, and 2016 were interpolated at 0.3 m resolution using the regularized spline with tension function (Mitasova and Mitas, 1993; Mitasova et al., 2005)⁶ from airborne lidar surveys collected by the NC Floodplain Mapping program and Fort Bragg. Unsupervised image classification⁷ was used to identify clusters of spectral reflectance⁸ in a timeseries of 1 meter resolution orthoimagery collected by the National Agriculture Imagery Program. The landcover maps were derived by fusing the classified lidar point clouds with the classified orthoimagery. Spatially variable soil erosion factors – k-factor, c-factor, manning's, and runoff rates – were derived from the landcover and soil maps. The dataset for this study is hosted at https://github.com/baharmon/landscape_evolution_dataset under the ODC Open Database License (ODbL). The data is derived from publicly available data from the US Army, USGS, USDA, Wake County GIS, NC Floodplain Mapping Program, and the NC State Climate Office.

We used the geomorphons method⁹ of automated landform classification based on the openness of terrain (Jasiewicz and Stepinski, 2013) and the difference between the digital elevation models to analyze the changing morphology of the study area (Figure 4d-f). The 2 m deep gully – its channels classified as valleys and its scour pits as depressions by geomorphons – has multiple mature branches and ends with a depositional fan. The gully has also developed depositional ridges beside the channels. Deep scour pits have developed where branches join the main channel and where the main channel has sharp bends. A new branch has begun to form in a knickzone classified as a mix of valleys and hollows on a grassy swale on the northeast side of the gully. Between 2012 and 2016 a depositional ridge has developed at the foot of this nascent branch where it would meet the main channel. The difference in elevation between 2012 and 2016 (Figure 4d) shows a deepening of the main channel by approximately 0.2 m and the scours pits by approximately 1 m, while depositional ridges have formed and grown up to approximately 1 m or more.

3.2 Simulations

We ran a sequence of simulations for the Patterson Branch Creek subwatershed study area to test dynamic and steady state flow regimes in the SIMWE, RUSLE3D, and USPED models (Table 3). We used RUSLE3D to simulate 120 min events with rainfall intensities of 50 mm hr⁻¹ for detachment capacity limited soil erosion regimes for both dynamic and steady state flow regimes using RUSLE3D (Figure 5a-c). We used USPED to simulate 120 min events with rainfall intensities of 50 mm hr⁻¹ for transport capacity limited soil erosion regimes for both dynamic and steady state flow regimes (Figure 5d-f). We used SIMWE to simulate 120 min events with rainfall intensities of 50 mm hr⁻¹ for erosion-deposition and detachment limited soil erosion regimes in steady state flow regimes (Figure 6). In all of the simulations we used a sink filling algorithm – an

⁶<https://grass.osgeo.org/grass74/manuals/v.surf.rst.html>

⁷<https://grass.osgeo.org/grass74/manuals/i.maxlik.html>

⁸<https://grass.osgeo.org/grass74/manuals/i.cluster.html>

⁹<https://grass.osgeo.org/grass74/manuals/r.geomorphon.html>

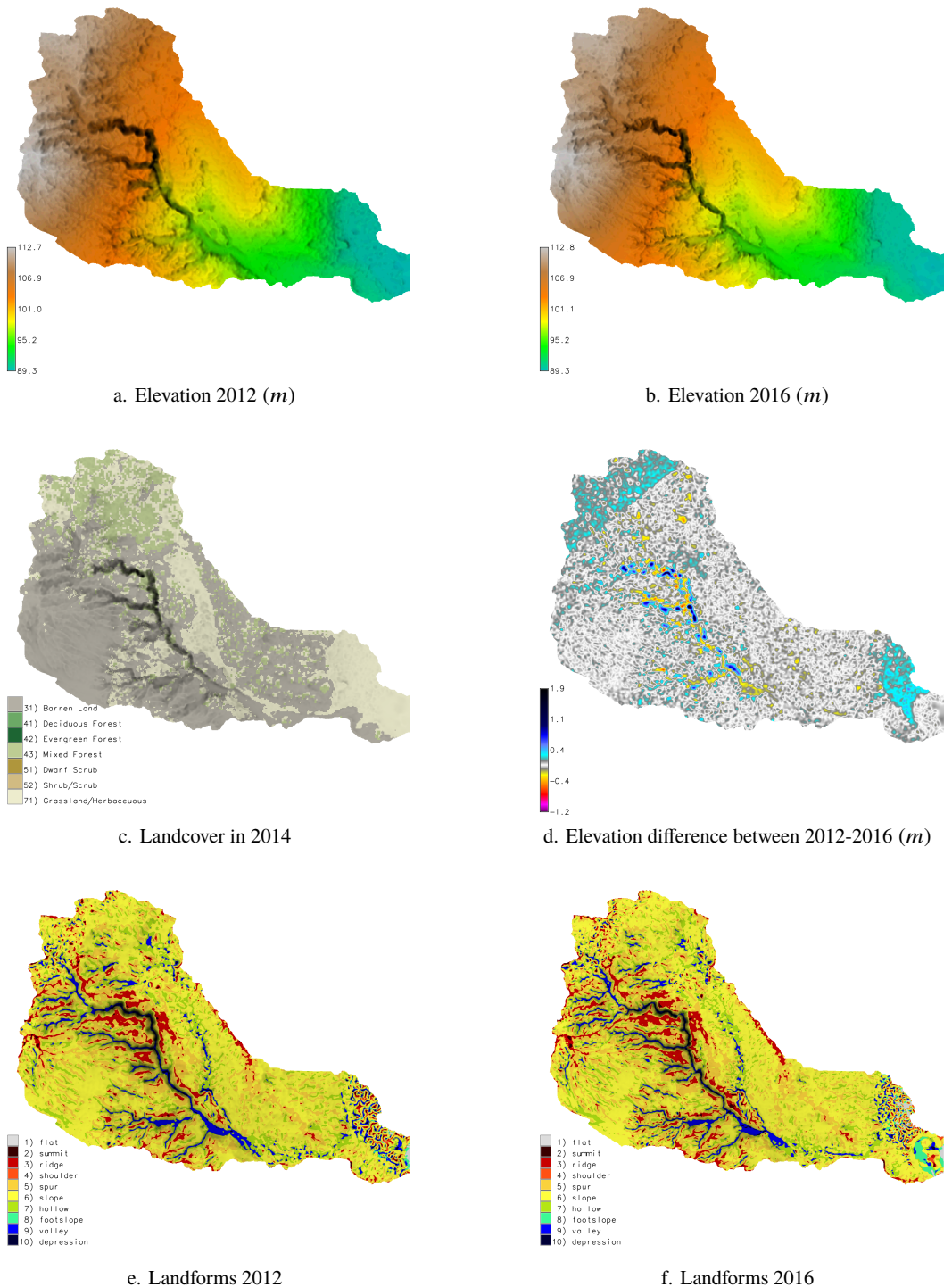


Figure 4. Subwatershed, Patterson Branch Creek, Fort Bragg, NC, USA

Table 3. Landscape evolution simulations

Dynamics	Model	Intensity	Duration	Interval	D_c	T_c	m	n	ρ_s	Threads	Runtime
Dynamic	RUSLE3D	50 mm hr^{-1}	120 min	3 min			0.4	1.3			2 min 36 s
Dynamic	USPED	50 mm hr^{-1}	120 min	3 min			1.5	1.2	1.6		3 min 14 s
Steady state	SIMWE	50 mm hr^{-1}	120 min	120 min	0.001				1.6	6	84 min 13 s
Steady state	SIMWE	25 mm hr^{-1}	120 min	120 min	0.0001	0.01			1.6	6	84 min 13 s

optional parameter in r.sim.terrain – to reduce the effects of positive feedback loops that cause the over-development of scour pits.

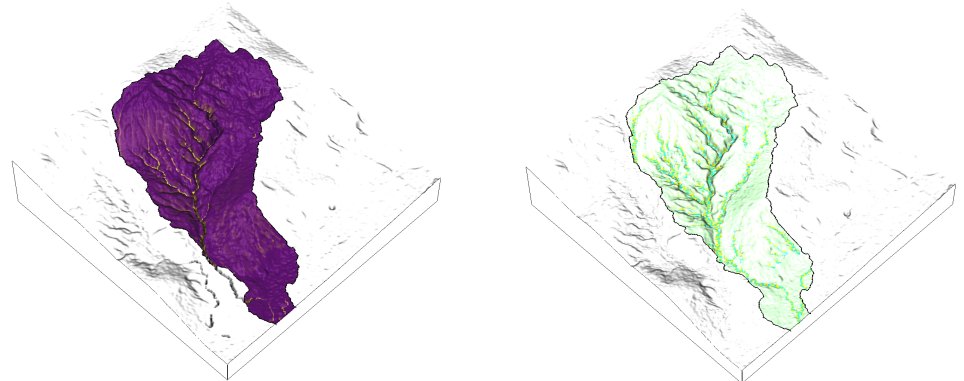
The simulations were automated and run in parallel using Python scripts that are available in the software repository. The simulations can be reproduced using these scripts and the study area dataset by following the instructions in the Open Science Framework repository at <https://osf.io/tf6yb/>. The simulations were run in GRASS GIS 7.4 on a desktop computer with 64-bit Ubuntu 16.04.4 LTS, 8 x 4.20 GHz Intel Core i7 7700K CPUs, and 32 GB RAM. Simulations using SIMWE are far more computationally intensive than RULSE3D or USPED, but support multi-threading when compiled with OpenMP. Dynamic simulations of RUSLE3D and USPED each took 3 min 14 s to run on a single thread, while steady state simulations for SIMWE each took 84 min 13 s running on 6 threads (Table 3).

The dynamic RUSLE3D simulation deepened the main channel of the gully, while the dynamic USPED simulation eroded the banks of the gully and deposited in channels causing the gully grow wider and shallower (Figure 5). As a detachment capacity limited model RUSLE3D's results were dominated by erosion and thus negative elevation change. RUSLE3D carved a deep incision in the main gully channel where water and sediment flow accumulated (Figure 5c). As a transport capacity limited model USPED generated a distributed pattern with both erosion and deposition and thus negative and positive elevation change. While USPED's pattern of elevation change was grainy and fragmented, it clearly captured the process of channel filling and widening expected for transport capacity limited soil erosion regime (Figure 5f).

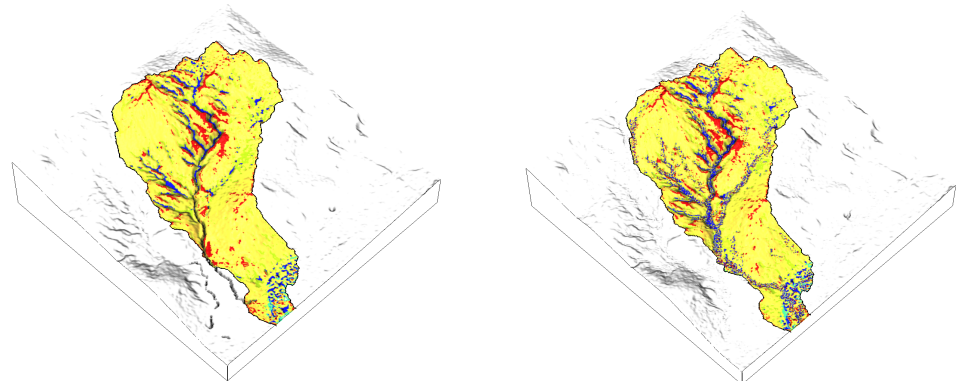
The steady state SIMWE simulations predicted more realistic patterns of landscape evolution (Figure 6). For transport limited and erosion-deposition regimes SIMWE simulated channel widening and the formation of depositional ridges along the centerline of the channel (Figure 6c). For a detachment limited soil erosion regime SIMWE simulated major erosion driving the development of the gully network (Figure 6f). The development of the nascent branch into a full fledged channel clearly demonstrated the process of gully formation.

4 Conclusions

...

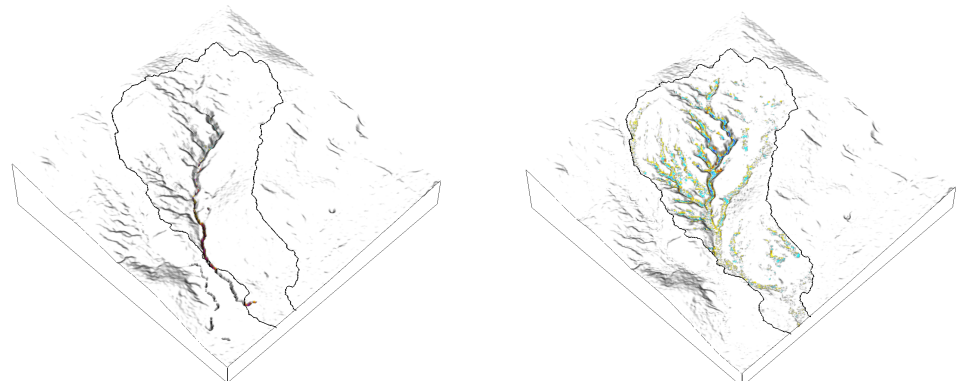


a. Dynamic RUSLE3D sediment flow ($kg\ m^{-2}\ s^{-1}$) d. Dynamic USPED erosion-deposition ($kg\ m^{-2}\ s^{-1}$)



b. Dynamic RUSLE3D landforms

e. Dynamic USPED landforms



c. Dynamic RUSLE3D net difference (m)

f. Dynamic USPED net difference (m)

Figure 5. Dynamic RUSLE3D and USPED simulations for a 120 min event with a rainfall intensity of $50\ mm\ hr^{-1}$

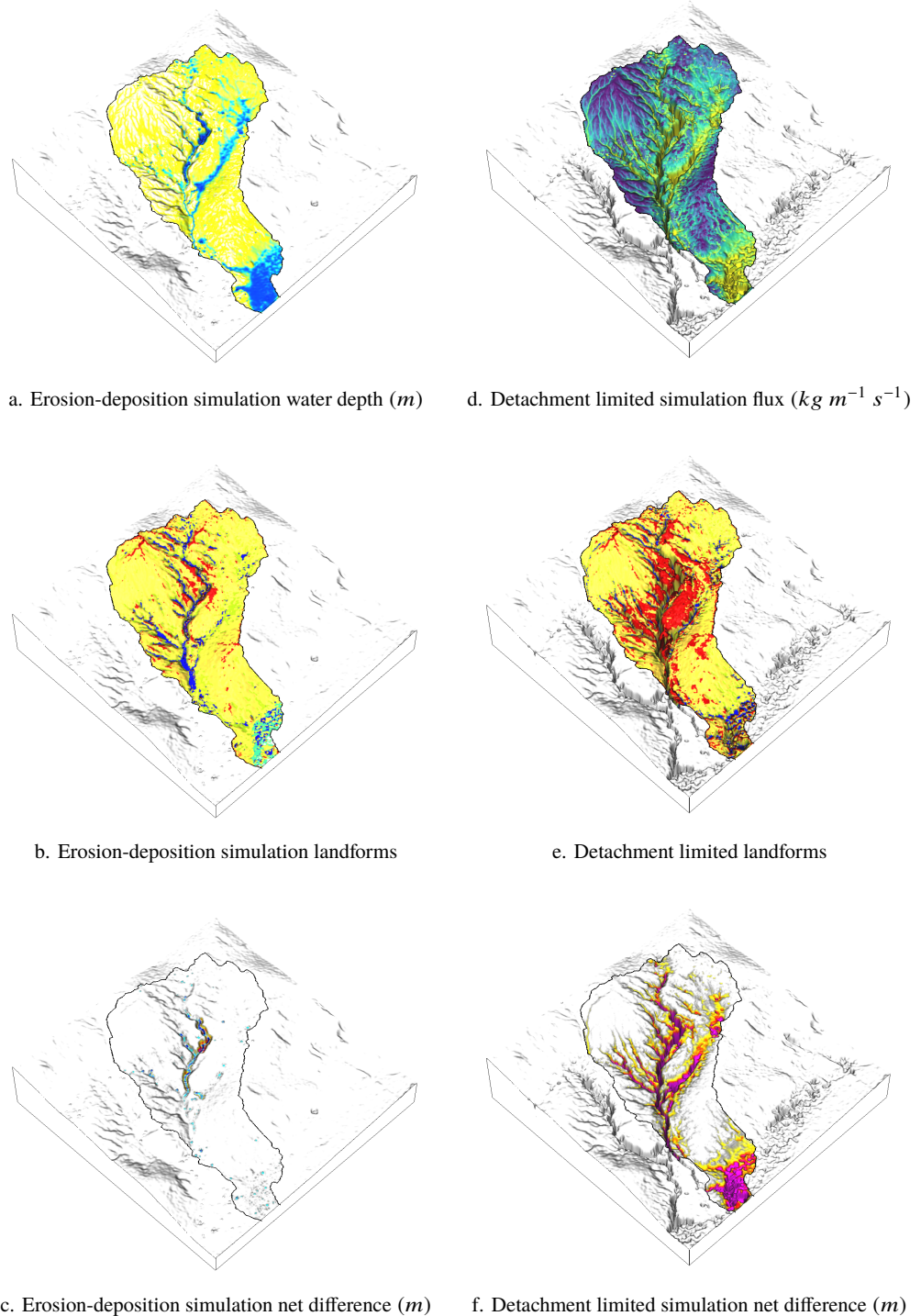


Figure 6. Steady state SIMWE simulations for 120 min events with rainfall intensities of $50\ mm\ hr^{-1}$ and $25\ mm\ hr^{-1}$

Code and data availability. The Python source code for the landscape evolution model is available on GitHub at https://github.com/baharmon/landscape_evolution under the GNU General Public License version 2. This repository also includes Python scripts for running and reproducing the simulations in this paper. The geospatial dataset for the study area is available on GitHub at https://github.com/baharmon/landscape_evolution_dataset under the Open Database License. The source code, scripts, data, and results are available on the Open Science Framework 5 at <https://osf.io/tf6yb/>.

Author contributions. Brendan Harmon developed the models, code, data, case studies, and text. Helena Mitasova contributed to the development of the models and case studies. Anna Petrasova and Vaclav Petras contributed to the development of the code.

Competing interests. The authors declare that they have no conflict of interest.

References

- Barton, C. M., Ullah, I., and Mitasova, H.: Computational Modeling and Neolithic Socioecological Dynamics: a Case Study from Southwest Asia, *American Antiquity*, 75, 364–386, <http://www.jstor.org/stable/25766199>, 2010.
- Bechet, J., Duc, J., Loyer, A., Jaboyedoff, M., Mathys, N., Malet, J. P., Klotz, S., Le Bouteiller, C., Rudaz, B., and Travelletti, J.: Detection
5 of seasonal cycles of erosion processes in a black marl gully from a time series of high-resolution digital elevation models (DEMs), *Earth Surface Dynamics*, 4, 781–798, <https://doi.org/10.5194/esurf-4-781-2016>, 2016.
- Brown, L. C. and Foster, G. R.: Storm Erosivity Using Idealized Intensity Distributions, *Transactions of the American Society of Agricultural Engineers*, 30, 0379 –0386, <https://doi.org/http://dx.doi.org/10.13031/2013.31957>, 1987.
- Dabney, S., Vieira, D., Bingner, R., Yoder, D., and Altinakar, M.: Modeling Agricultural Sheet , Rill and Ephemeral Gully Erosion, in: ICHE
10 2014. Proceedings of the 11th International Conference on Hydroscience & Engineering, pp. 1119–1126, Karlsruhe, 2014.
- Dennis C. Flanagan, James R. Frankenberger, Thomas A. Cochrane, Chris S. Renschler, and William J. Elliot: Geospatial Application of the Water Erosion Prediction Project (WEPP) Model, *Transactions of the ASABE*, 56, 591–601, <https://doi.org/10.13031/2013.42681>, <https://www.fs.usda.gov/treesearch/pubs/43830>, 2013.
- Ehlschlaeger, C.: Using the A^T Search Algorithm to Develop Hydrologic Models from Digital Elevation Data, in: Proceedings of International
15 Geographic Information Systems (IGIS) Symposium '89, pp. 275–281, Baltimore, MD, 1989.
- Guertin, D. P., Goodrich, D. C., Burns, I. S., Korgaonkar, Y., Barlow, J., Sheppard, B. S., Unkrich, C., and Kepner, W.: Automated Geospatial Watershed Assessment Tool (AGWA), <https://doi.org/10.1061/9780784479322.012>, <https://ascelibrary.org/doi/abs/10.1061/9780784479322.012>, 2015.
- Hobley, D. E., Adams, J. M., Siddhartha Nudurupati, S., Hutton, E. W., Gasparini, N. M., Istanbulluoglu, E., and Tucker, G. E.: Creative
20 computing with Landlab: An open-source toolkit for building, coupling, and exploring two-dimensional numerical models of Earth-surface dynamics, *Earth Surface Dynamics*, 5, 21–46, <https://doi.org/10.5194/esurf-5-21-2017>, 2017.
- Jasiewicz, J. and Stepinski, T. F.: Geomorphons - a pattern recognition approach to classification and mapping of landforms, *Geomorphology*, 182, 147–156, <https://doi.org/10.1016/j.geomorph.2012.11.005>, 2013.
- Koco, Š.: Simulation of gully erosion using the SIMWE model and GIS, *Landsurface Analysis*, 17, 81–86, 2011.
- Malik, I.: Dating of small gully formation and establishing erosion rates in old gullies under forest by means of anatomical changes in exposed tree roots (Southern Poland), *Geomorphology*, 93, 421–436, <https://doi.org/10.1016/j.geomorph.2007.03.007>, 2008.
- Metz, M., Mitasova, H., and Harmon, R. S.: Fast Stream Extraction from Large , Radar- Based Elevation Models with Variable Level of Detail, pp. 237–242, 2009.
- Mitas, L. and Mitasova, H.: Distributed soil erosion simulation for effective erosion prevention, *Water Resources Research*, 34, 505–516,
30 <https://doi.org/10.1029/97wr03347>, 1998.
- Mitasova, H. and Mitas, L.: Interpolation by regularized spline with tension: I. Theory and implementation, *Mathematical Geology*, 25, 641–655, <https://doi.org/10.1007/BF00893171>, 1993.
- Mitasova, H. and Mitas, L.: Multiscale soil erosion simulations for land use management, in: *Landscape erosion and evolution modeling*, edited by Harmon, R. S. and Doe, W. W., chap. 11, pp. 321–347, Springer, Boston, MA, https://doi.org/10.1007/978-1-4615-0575-4_11,
35 <http://citeseerx.ist.psu.edu/viewdoc/download?doi=10.1.1.69.5171&rep=rep1&type=pdf>, 2001.

- Mitasova, H., Hofierka, J., Zlocha, M., and Iverson, L. R.: Modelling topographic potential for erosion and deposition using GIS, International Journal of Geographical Information Science, 10, 629–641, <https://doi.org/10.1080/02693799608902101>, <http://dx.doi.org/10.1080/02693799608902101>, 1996.
- Mitasova, H., Thaxton, C., Hofierka, J., McLaughlin, R., Moore, A., and Mitas, L.: Path sampling method for modeling overland water flow, sediment transport, and short term terrain evolution in Open Source GIS, Developments in Water Science, 55, 1479–1490, [https://doi.org/10.1016/S0167-5648\(04\)80159-X](https://doi.org/10.1016/S0167-5648(04)80159-X), 2004.
- Mitasova, H., Mitas, L., and Harmon, R. S.: Simultaneous spline approximation and topographic analysis for lidar elevation data in open-source GIS, IEEE Geoscience and Remote Sensing Letters, 2, 375–379, <https://doi.org/10.1109/LGRS.2005.848533>, 2005.
- Mitasova, H., Barton, M., Ullah, I., Hofierka, J., and Harmon, R.: 3.9 GIS-Based Soil Erosion Modeling, in: Treatise on Geomorphology, edited by Shroder, J. F., chap. 3.9, pp. 228–258, Elsevier, San Diego, California, USA, <https://doi.org/10.1016/B978-0-12-374739-6.00052-X>, <http://www.sciencedirect.com/science/article/pii/B978012374739600052X>, 2013.
- Renard, K. G., Foster, G. R., Weesies, G. A., McCool, D. K., and Yoder, D. C.: Predicting soil erosion by water: a guide to conservation planning with the Revised Universal Soil Loss Equation (RUSLE), Tech. Rep. 703, US Government Printing Office, Washington, DC, https://www.ars.usda.gov/ARSUserFiles/64080530/rusle/ah_703.pdf, 1997.
- Shobe, C. M., Tucker, G. E., and Barnhart, K. R.: The SPACE 1.0 model: A Landlab component for 2-D calculation of sediment transport, bedrock erosion, and landscape evolution, Geoscientific Model Development, 10, 4577–4604, <https://doi.org/10.5194/gmd-10-4577-2017>, 2017.
- Sorrie, B. A.: An Inventory of the Significant Natural Areas of Hoke County, North Carolina, Tech. rep., North Carolina Natural Heritage Program, <https://www.denix.osd.mil/nr/priorities/invasivespecies/reports/an-inventory-of-the-significant-natural-areas-of-hoke-county-north-carolina-september-2004/>, 2004.
- Sorrie, B. A., Gray, J. B., and Crutchfield, P. J.: The Vascular Flora of the Longleaf Pine Ecosystem of Fort Bragg and Weymouth Woods, North Carolina, Castanea, 71, 129–161, <https://doi.org/10.2179/05-02.1>, 2006.
- Starek, M. J., Mitasova, H., Hardin, E., Weaver, K., Overton, M., and Harmon, R. S.: Modeling and analysis of landscape evolution using airborne , terrestrial , and laboratory laser scanning, Geosphere, 7, 1340–1356, <https://doi.org/10.1130/GES00699.1>, 2011.
- Temme, A., Schoorl, J., Claessens, L., and Veldkamp, A.: 2.13 Quantitative Modeling of Landscape Evolution, vol. 2, Elsevier Ltd., <https://doi.org/10.1016/B978-0-12-374739-6.00039-7>, <http://linkinghub.elsevier.com/retrieve/pii/B9780123747396000397>, 2013.
- Thaxton, C. S.: Investigations of grain size dependent sediment transport phenomena on multiple scales, Phd, North Carolina State University, <http://www.lib.ncsu.edu/resolver/1840.16/3339>, 2004.
- Thomas, J. T., Iverson, N. R., Burkart, M. R., and Kramer, L. A.: Long-term growth of a valley-bottom gully, Western Iowa, Earth Surface Processes and Landforms, 29, 995–1009, <https://doi.org/10.1002/esp.1084>, 2004.
- Tucker, G., Lancaster, S., Gasparini, N., and Bras, R.: The channel-hillslope integrated landscape development model (CHILD), in: Landscape erosion and evolution modeling, pp. 349–388, Springer, Boston, MA, https://doi.org/10.1007/978-1-4615-0575-4_12, 2001.
- Willgoose, G.: Mathematical Modeling of Whole Landscape Evolution, Annual Review of Earth and Planetary Sciences, 33, 443–459, <https://doi.org/10.1146/annurev.earth.33.092203.122610>, <http://www.annualreviews.org/doi/10.1146/annurev.earth.33.092203.122610>, 2005.
- Wischmeier, W. H., Smith, D. D., Science, U. S., Administration, E., and Station, P. U. A. E.: Predicting Rainfall Erosion Losses: A Guide to Conservation Planning, Tech. rep., Washington, D.C., <https://naldc.nal.usda.gov/download/CAT79706928/>, 1978.